Robotics and Autonomous Systems 59 (2011) 57–64

Contents lists available at ScienceDirect

Robotics and Autonomous Systems

journal homepage: www.elsevier.com/locate/robot

A control strategy for platoons of differential drive wheeled mobile robot

Gregor Klančar *, Drago Matko, Sašo Blažič

Laboratory of Modelling, Simulation and Control, Faculty of Electrical Engineering, University of Ljubljana, Tržaška 25, SI-1000 Ljubljana, Slovenia

ARTICLE INFO

Article history:
Received 9 November 2009
Received in revised form
9 December 2010
Accepted 13 December 2010
Available online 22 December 2010

Keywords:
Mobile robots
Platoon
Reactive multi-Agent
Path following control

ABSTRACT

The strategy for the control of vehicle platooning is proposed and tested on different mobile robot platforms. The decentralized platooning is considered, i.e. a virtual train of vehicles where each vehicle is autonomous and decides on its motion based on its own perceptions. The following vehicle only has information about its distance and azimuth to the leading vehicle. Its position is determined using odometry. The reference position and the orientation of the following vehicle are determined by the estimated path of the leading vehicle in a parametric polynomial form. The parameters of the polynomials are determined using the least-squares method. This parametric reference path is also used to determine the feed-forward part and to suppress tracking errors by a feed-back part of the applied globally stable nonlinear control law. The results of the experiment and simulations demonstrate the applicability of the proposed algorithm for vehicle platoons.

© 2010 Elsevier B.V. All rights reserved.

1. Introduction

Vehicle platoon systems are a promising approach for new transportation systems [1] because of their innovative capabilities. Their main goals when applied to passenger cars are an increase in the vehicle density on the highway (i.e. avoiding traffic jams), and security improvements in new passenger transportation services in urban environments thanks to automated or semi-automated driving assistance (adaptive cruise control, obstacle detection and avoidance, automatic car parking, etc.). Most of these platooning systems are based on a linear configuration (i.e. a virtual train of vehicles). A basic problem in platoon systems is the control of the vectorial inter-vehicle distance. Some of the most spread approaches are based on automatic control. In this frame, the control of global platoon geometry has been decomposed into different sub-problems: longitudinal control (distance regulation), lateral control (angle regulation), integrated lateral and longitudinal control and merge/split capabilities. Most of the lateral or longitudinal control proposals are based on PID control [1–4] or other regulation-loop-based methods such as control based on linearization methods in [5] or fuzzy logic control in [6,7]. From the industrial point of view, Automatic Cruise Control (ACC), introduced by Mercedes-Benz in 1998, deals with longitudinal control and Lane Keeping Assist System (AFIL), developed by Citroen, deals with lateral control. Integrated longitudinal and lateral control has also attracted research as in [8,9] and in [10,11] where physics-inspired models were used or Multi-Agent System modelling as in [12]. Finally, platoon systems should have merge and split capabilities. Merge consists in adding a vehicle to the train and split consists in removing a vehicle from the train. In the literature, examples can be found dealing with merging and splitting from an already well formed linear platoon running on a highway [13,14].

Regarding the perception vehicles platoons classify into two main categories: local approaches [15,16] and global approaches [17,18]. Local approaches usually react to current relative sensor information only as opposed to global approaches where global positions of vehicles as well as the course of the reference path are known.

In this work research results about a platoon of nonholonomic vehicles using a nonlinear globally stable trajectory tracking control law are presented. The novelties of the proposed approach with respect to our previously published work [19] are: application of the nonlinear globally stable control law in a platoon of nonholonomic vehicles, completely local approach where only the leader relative position is required (in [19] also the global robot orientation measurement (e.g. compass) needs to be known), comparison of platoon approach using constant inter-vehicle spacing and approach using constant inter-vehicle time (time-headway), and error propagation analysis in the platoon which gives some measure on limitations of the used strategy and validation of the approach on experiments with local stereo camera sensor. The vehicle platooning control strategy relies on relative information to preceding vehicles only, therefore no explicit inter-vehicle data exchange and global information (such as GPS) are required. The important advantage here is that relative information can be measured with low cost sensor sets.

The aspects of integration of merging and splitting capabilities and obstacle avoidance to the platoon are already discussed in our previous work [19]. The main difference of the proposed approach

* Corresponding author. Tel.: +386 1 4768764; fax: +386 1 4264631.
E-mail address: gregor.klancar@fe.uni-lj.si (G. Klančar).

0921-8890/$ – see front matter © 2010 Elsevier B.V. All rights reserved.
doi:10.1016/j.robot.2010.12.002

compared to other local approaches is the capability of each vehicle to estimate the trajectory of the vehicle in front of it and follow this estimated trajectory instead of reacting to current sensor information only. The trajectory shape can be arbitrary continuous curve.

Mobile robots used in the work are nonholonomic systems which have motion limitations resulting from their kinematic model. Nonlinear globally stable control [20,21] is applied to follow an arbitrary reference path with a predefined velocity profile. The control structure consists of feed-forward control part and feed-back control part. The feed-forward part is calculated from the known trajectory while the feed-back control part takes care of small tracking-error corrections due to disturbances, noise and unmodelled dynamics.

The paper is organized as follows: The trajectory tracking control law that can be applied to nonholonomic systems is presented in Section 2. The application of the proposed control law to platoon systems is derived in Section 3. The error accumulation effect through the number of vehicles in the platoon for the proposed approach is analyzed in Section 4. The results of the test on different mobile robot platforms are presented in Section 5.

2. Trajectory tracking for nonholonomic vehicles

The kinematic model of the vehicle with differential drive is given as follows

$$\begin{bmatrix}\dot{x}(t)\\ \dot{y}(t)\\ \dot{\theta}(t)\end{bmatrix} = \begin{bmatrix}\cos\theta(t) & 0\\ \sin\theta(t) & 0\\ 0 & 1\end{bmatrix}\cdot\begin{bmatrix}v(t)\\ \omega(t)\end{bmatrix} \tag{1}$$

where v and ω are the tangential and the angular velocities of the vehicle (following vehicle in Fig. 1), respectively.

It is very easy to show that the system (1) is flat [22] with flat outputs being x and y. The flatness property enables the existence of the open-loop control that achieves perfect tracking in the ideal case of the vehicle dynamics described by (1). For a given smooth reference trajectory $(x_r(t), y_r(t))$ defined in the time interval $t \in [0, T]$ the open-loop (or flatness-based) control (v_{ff} and ω_{ff}) can be derived as

$$v_{ff}(t) = \sqrt{\dot{x}_r^2(t) + \dot{y}_r^2(t)} \tag{2}$$

$$\omega_{ff}(t) = \frac{\dot{x}_r(t)\ddot{y}_r(t) - \dot{y}_r(t)\ddot{x}_r(t)}{\dot{x}_r^2(t) + \dot{y}_r^2(t)} = v_{ff}(t)\kappa(t) \tag{3}$$

where $\kappa(t)$ is the reference path's curvature. The necessary condition in the path-design procedure is a twice-differentiable path and a nonzero tangential velocity $v_{ff}(t) \neq 0$ at each time instant. The reference robot pose is then given by $q_r(t) = [x_r(t), y_r(t), \theta_r(t)]^T$, where $\theta_r(t)$ is trajectory tangent angle in point $(x_r(t), y_r(t))$. Taking into account a given reference robot pose and the controls from Eqs. (2) and (3), the following relation can be obtained:

$$\begin{bmatrix}\dot{x}_r(t)\\ \dot{y}_r(t)\\ \dot{\theta}_r(t)\end{bmatrix} = \begin{bmatrix}\cos\theta_r(t) & 0\\ \sin\theta_r(t) & 0\\ 0 & 1\end{bmatrix}\cdot\begin{bmatrix}v_{ff}(t)\\ \omega_{ff}(t)\end{bmatrix}. \tag{4}$$

In Fig. 1 the reference vehicle is an imaginary vehicle that ideally follows the reference path. In contrast, the real vehicle (when compared to the reference vehicle) has some error when following the reference path. The trajectory tracking error, expressed in terms of the following vehicle, as shown in Fig. 1, is given by

$$e(t) = \begin{bmatrix}e_x(t)\\ e_y(t)\\ e_\theta(t)\end{bmatrix} = \begin{bmatrix}\cos\theta(t) & \sin\theta(t) & 0\\ -\sin\theta(t) & \cos\theta(t) & 0\\ 0 & 0 & 1\end{bmatrix}\cdot\begin{bmatrix}x_r(t) - x(t)\\ y_r(t) - y(t)\\ \theta_r(t) - \theta(t)\end{bmatrix}. \tag{5}$$

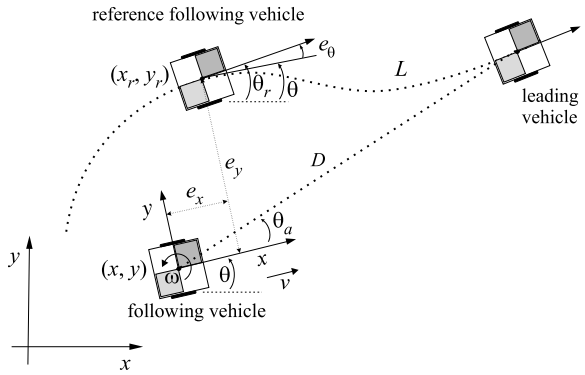

Fig. 1. Illustration of the error transformation where the following vehicle follows the path of the leading vehicle at distance L.

Differentiating Eq. (5) with respect to time and taking into account the kinematic model given by Eq. (1), and the equivalent kinematic model of the reference vehicle given by Eq. (4), the following nonlinear error model of the system is obtained:

$$\begin{aligned}\dot{e}_x(t) &= \omega(t)e_y(t) + v_{ff}(t)\cos(e_\theta(t)) - v(t)\\ \dot{e}_y(t) &= -\omega(t)e_x(t) + v_{ff}(t)\sin(e_\theta(t))\\ \dot{e}_\theta(t) &= \omega_{ff}(t) - \omega(t).\end{aligned} \tag{6}$$

The control algorithm should be designed to force the vehicle follow the reference path precisely. The nonlinear controller design approach as proposed in [21,20] is used where global asymptotic stability is shown using appropriate Lyapunov function [23]. The nonlinear control law is as follows

$$\begin{aligned}v(t) &= v_{ff}(t)\cos e_\theta(t) + k_x(t)e_x(t)\\ \omega(t) &= \omega_{ff}(t) + k_y v_{ff}(t)\frac{\sin e_\theta(t)}{e_\theta(t)}e_y(t) + k_\theta(t)e_\theta(t)\end{aligned} \tag{7}$$

where k_y is a positive constant, while $k_x(t)$ and $k_\theta(t)$ are continuous positive bounded functions that will be discussed later on in the paper.

3. Linear platoon control strategy

In the proposed control strategy each following vehicle measures the distance D and the azimuth θ_a (relative to its own orientation, see Fig. 1) to its leading vehicle. No additional data communication between the leading and following vehicles is available. The distance D and the azimuth θ_a are obtained from local sensor sets (laser range scanner or stereo camera). No other global information sensors (e.g. GPS) are required. The only assumption is that the path of the first robot is feasible to all the following robots which may have different kinematic and dynamic constraints. All the positions are treated in a coordinate system that is fixed to the ground. The following vehicle determines its own pose using odometry. Having the current pose $\mathbf{X}(k\Delta t) = [x(k\Delta t), y(k\Delta t), \theta(k\Delta t)]^T$, the pose in the next sample is determined by Euler integration

$$\mathbf{X}((k+1)\Delta t) = \mathbf{X}(k\Delta t) + \Delta t\begin{bmatrix}\cos(\theta(k\Delta t)) & 0\\ \sin(\theta(k\Delta t)) & 0\\ 0 & 1\end{bmatrix}\begin{bmatrix}v(k\Delta t)\\ \omega(k\Delta t)\end{bmatrix} \tag{8}$$

where $v(k\Delta t)$ and $\omega(k\Delta t)$ are the current translational and angular speed of the vehicle, and Δt is the sample time. However the vehicles pose estimation given in (8) is not limited to differential drive kinematics only. For other robot types (e.g. Ackerman steering) relation (8) needs to be updated with robot kinematic as follows

$$\mathbf{X}((k+1)\Delta t) = \mathbf{X}(k\Delta t) + \Delta t\dot{\mathbf{X}}(k\Delta t)$$

where $\dot{\mathbf{X}}(k\Delta t) = \mathbf{f}(\mathbf{X}(k\Delta t), \mathbf{U}(k\Delta t))$ is the robot kinematic model and $\mathbf{U}(k\Delta t)$ are the robot commands. As shown in [19] the method of integration and the associated errors in the accuracy of the absolute position are not significant since only the relative position information among vehicles (D and θ_a) is important. The latter is always obtained from accurate relative sensors sets therefore the integration error and errors due to wheels slipping does not influence the servoing accuracy noticeably.

The path of the leading vehicle $\mathbf{X}_h(k\Delta t) = [x_h(k\Delta t), y_h(k\Delta t)]^T$ is calculated by the following vehicle using its current position and the measurements of the distance D and the azimuth θ_a as follows:

$$\mathbf{X}_h(k\Delta t) = \begin{bmatrix} x(k\Delta t) \\ y(k\Delta t) \end{bmatrix} + \begin{bmatrix} \cos\big(\theta(k\Delta t) + \theta_a(k\Delta t)\big) \\ \sin\big(\theta(k\Delta t) + \theta_a(k\Delta t)\big) \end{bmatrix} D(k\Delta t). \quad (9)$$

This information is stored in the memory and represented in parametric form (with the parameter k—related to the time $t = k\Delta t$). Intermediate points are obtained by means of linear interpolation

$$\mathbf{X}_h(t) = \mathbf{X}_h(k\Delta t) + \frac{t - k\Delta t}{\Delta t}[\mathbf{X}_h\big((k+1)\Delta t\big) - \mathbf{X}_h(k\Delta t)] \quad k\Delta t \le t < (k+1)\Delta t. \quad (10)$$

To estimate the leading robot pose the kinematic model of the leading robot is not required and is therefore unknown to the following robot.

Each following vehicle must track its leading vehicle (vehicle in front) path either by constant inter-vehicle spacing policy or by constant inter-vehicle time policy. Constant spacing approach is compared to constant time approach more vulnerable to error accumulation through the number of vehicles and consequently to string stability problem but it has some practical benefits relating to the vehicle size which can be considered implicitly by selecting the desired inter-vehicle safety distance. Therefore a combination of both approaches is usually used in applications. In the following section both basic approaches are implemented in the platoon control strategy.

3.1. Constant distance approach

The following vehicle is supposed to track the leading vehicle at a distance L—measured on the path of the leading vehicle as already proposed in our previous work [19]. To estimate the path length, the distance function $L_h(t)$ that gives the distance travelled by the leading vehicle is defined as

$$L_h(t) = \int_0^t \sqrt{\dot{x}_h^2(\tau) + \dot{y}_h^2(\tau)}\,\mathrm{d}\tau. \quad (11)$$

The following vehicle should track the leading vehicle (9) at a distance L, i.e. at the current time t_0 it should follow the position of the leading vehicle at $t = T$, where T is defined by

$$L_h(T) = \begin{cases} L_h(t_0) - L & L_h(t_0) \ge L \\ 0 & L_h(t_0) < L. \end{cases} \quad (12)$$

More details on constant distance approach can be found in [19].

3.2. Constant time approach

The following vehicle is supposed to track the leading vehicle path with constant time delay T_f which means that inter-vehicle distance $L(t)$ varies depending on current leader vehicle speed $v_h(t)$. Two extreme situations may appear as follows $\lim_{v_h \to 0} L(t) = 0$ and $\lim_{v_h \to \infty} L(t) = \infty$ therefore this approach is appropriate for situations where v_h is bounded: $0 < v_{h\min} \le v_h(t) \le v_{h\max}$.

The appropriate reference point on the leading vehicle path (9) is obtained as follows: at the current time t_0 the following vehicle should follow the position of the leading vehicle at $t = t_0 - T_f$. The reference position at time t is calculated using relation (10).

3.3. Reference pose and reference velocity estimation

To implement control law from (7) also first and second order derivatives of the path in the determined reference point need to be estimated. This is done by estimating path shape around the reference point by parametric polynomial form. This step also suppresses noise from the sensors due to data averaging.

To estimate path shape around the reference point the path of the leading vehicle is expressed in the parametric polynomial form in the interval $[t_s, t_e]$ where $T \in [t_s, t_e]$:

$$\begin{aligned} \hat{x}_h(t) &= a_2^x t^2 + a_1^x t + a_0^x \\ \hat{y}_h(t) &= a_2^y t^2 + a_1^y t + a_0^y \end{aligned} \quad (13)$$

where the functions $\hat{x}_h(t)$ and $\hat{y}_h(t)$ approximate the functions $x_h(t)$ and $y_h(t)$, respectively, in the interval $[t_s, t_e]$. The coefficients of the polynomials a_i^x and a_i^y ($i = 0, 1, 2$) are calculated using the least-squares method with at least three samples around the time T (six points were used in our experiments). The second order polynomials (13) can successfully approximate the small piece of the leading vehicle path (consisting only of a few samples around the time T) because of the small sampling time Δt compared to the vehicle driving dynamics. As already mentioned, the position error due to dead reckoning (navigation with odometry) is not critical in the proposed algorithm because only the relative information (D and θ_a) between the leading and the following vehicle is important. Moreover, in the short time window (a few samples around T) where polynomials (13) are estimated, these errors do not significantly affect the trajectory estimation.

The reference pose (in Fig. 1 denoted as the reference vehicle) of the following vehicle at the current time t_0 is determined using

$$\begin{bmatrix} x_r(t_0) \\ y_r(t_0) \\ \theta_r(t_0) \end{bmatrix} = \begin{bmatrix} \hat{x}_h(T) \\ \hat{y}_h(T) \\ \hat{\theta}_h(T) \end{bmatrix} = \begin{bmatrix} a_2^x T^2 + a_1^x T + a_0^x \\ a_2^y T^2 + a_1^y T + a_0^y \\ \arctan \dfrac{2a_2^y T + a_1^y}{2a_2^x T + a_1^x} + \sigma \cdot \mathrm{sign}(2a_2^y T + a_1^y)\pi \end{bmatrix} \quad (14)$$

where $\sigma = 1$ if $(2a_2^x T + a_1^x) < 0$ and $\sigma = 0$ if $(2a_2^x T + a_1^x) \ge 0$ and sign$(\cdot)$ is signum function. The control law (7) is used for reference tracking (following the path of the leading robot) in a linear platoon. The required error vector is given according to Eq. (5) and the feed-forward tangential and angular velocities of the reference vehicle needed in (7) are calculated by

$$v_{ff}(t_0) = \sqrt{(2a_2^x T + a_1^x)^2 + (2a_2^y T + a_1^y)^2} \quad (15)$$

and

$$\omega_{ff}(t_0) = \frac{(2a_2^x T + a_1^x) \times 2a_2^y - (2a_2^y T + a_1^y) \times 2a_2^x}{(2a_2^x T + a_1^x)^2 + (2a_2^y T + a_1^y)^2} \quad (16)$$

respectively.

4. Error propagation analysis

In the following the effect of error accumulation through the number of vehicles in the platoon for the proposed approach is analyzed. This phenomenon is very much related to the string

stability. A platoon of vehicles is string stable if the range errors decrease as they propagate along the vehicle stream [18]. It has been shown that vehicle-to-vehicle communication is necessary to achieve string stability with constant inter-vehicle spacing [18]. However, platoon with constant time-headway could be string stable without additional communication.

In the following the error propagation through the platoon is analyzed. Let us imagine a virtual platoon where vehicles drive with zero time-headway. This means that the following vehicle just tries to follow the preceding vehicle path (without any delay). The reference for the following vehicle is actually the output of the preceding one. If the control is designed in a way that the tracking error of a single vehicle decreases with time from some initial value, the error will also decrease through the vehicles in the platoon. This statement also holds when the vehicles try to follow the path of the preceding vehicles with some time-headway. The only difference is that their reference is defined as a delayed measurement of the preceding vehicle in such case.

In practical implementations the measurements are corrupted by persistent disturbances. If the state transition matrix elements of the error model are less than 1 at all times, the errors are not amplified through the system. The output of a nth vehicle in the platoon does not follow the reference pose of the first vehicle asymptotically but the error remains bounded if the number of vehicles is finite. In the following the state transition matrix elements of the error model will be analyzed.

Inserting (7) into (6), the following error model is obtained:

$$\begin{aligned}\dot{e}_x &= \omega_{ff} e_y + k_y v_{ff} \frac{\sin e_\theta}{e_\theta} e_y^2 + k_\theta e_y e_\theta - k_x e_x\\ \dot{e}_y &= -\omega_{ff} e_x - k_y v_{ff} \frac{\sin e_\theta}{e_\theta} e_x e_y - k_\theta e_x e_\theta + v_{ff} \sin e_\theta\\ \dot{e}_\theta &= -k_y v_{ff} \frac{\sin e_\theta}{e_\theta} e_y - k_\theta e_\theta.\end{aligned} \tag{17}$$

It is impossible to analytically calculate the state transition matrix of the nonlinear error system in (17) for the arbitrary values of the control gains k_x, k_y, and k_θ. In our case the gain scheduling proposed in [21,20] is used:

$$\begin{aligned}&k_x(t) = 2\zeta\omega_n(t), \qquad \omega_n(t) = \sqrt{\omega_{ff}^2(t) + g v_{ff}^2(t)}\\ &k_y = g = \text{const.}\\ &k_\theta(t) = 2\zeta\omega_n(t), \qquad \omega_n(t) = \sqrt{\omega_{ff}^2(t) + g v_{ff}^2(t)}\end{aligned} \tag{18}$$

where $g > 0$ is an additional tuning parameter and $\zeta \in (0, 1)$ is a desired damping coefficient.

Inserting (18) into (17) the nonlinear error model of the controlled system can be obtained. For the purpose of analysis a simpler model will be used which is obtained by linearization of the nonlinear error model around the zero-error state (in this case the terms with products among states drop out while $\sin e_\theta$ is replaced by e_θ):

$$\dot{e}(t) = \begin{bmatrix} -2\zeta\omega_n(t) & \omega_{ff}(t) & 0\\ -\omega_{ff}(t) & 0 & v_{ff}(t)\\ 0 & -g v_{ff}(t) & -2\zeta\omega_n(t)\end{bmatrix} e(t) = A(t)e(t) \tag{19}$$

where the time-varying matrix $A(t)$ has been introduced.

The gain scheduling (18) was originally proposed for linear controller design [21,20] and gives time-varying (but with constant damping) eigenvalues of $A(t)$: $-2\zeta\omega_n(t)$, $-\zeta\omega_n(t) \pm j\omega_n(t)\sqrt{(1-\zeta^2)}$. Such choice of parameters can also be used in nonlinear control law (7) as it does not violate the constraints on controller gains, but the eigenvalues interpretation is preserved. Note that characteristic frequency $\omega_n(t)$ has to be time-varying (it changes as governed by $v_{ff}(t)$ and $\omega_{ff}(t)$) to prevent control gains grow unbounded when the robot velocity tends to 0.

The problem of error propagation will first be solved for one robot driving along simple trajectories (straight lines and circles). If v_{ff} and ω_{ff} are constant, then ω_n and A are also constant due to (18) and (19) can be solved analytically:

$$e(t) = \mathrm{e}^{At} e(0) = \Phi(t) e(0). \tag{20}$$

The elements of the obtained state transition matrix $\Phi(t)$ are as follows:

$$\begin{aligned}\phi_{1,1}(t) &= -\left(\frac{\omega_{ff}}{\omega_n}\right)^2 \mathrm{e}^{-\omega_r t}\\ &\quad\times\left(\frac{\zeta}{\sqrt{1-\zeta^2}}\sin(\omega_i t) - \cos(\omega_i t) + \mathrm{e}^{-\omega_r t}\right) + \mathrm{e}^{-2\omega_r t}\\ \phi_{1,2}(t) &= \frac{\frac{\omega_{ff}}{\omega_n}\mathrm{e}^{-\omega_r t}\sin(\omega_i t)}{\sqrt{1-\zeta^2}}\\ \phi_{1,3}(t) &= \frac{\omega_{ff}}{\omega_n}\frac{v_{ff}}{\omega_n}\mathrm{e}^{-\omega_r t}\\ &\quad\times\left(\frac{\zeta}{\sqrt{1-\zeta^2}}\sin(\omega_i t) - \cos(\omega_i t) + \mathrm{e}^{-\omega_r t}\right)\\ \phi_{2,1}(t) &= -\frac{\frac{\omega_{ff}}{\omega_n}\mathrm{e}^{-\omega_r t}\sin(\omega_i t)}{\sqrt{1-\zeta^2}}\\ \phi_{2,2}(t) &= \mathrm{e}^{-\omega_r t}\left(\frac{\zeta}{\sqrt{1-\zeta^2}}\sin(\omega_i t) + \cos(\omega_i t)\right)\\ \phi_{2,3}(t) &= \frac{\frac{v_{ff}}{\omega_n}\mathrm{e}^{-\omega_r t}\sin(\omega_i t)}{\sqrt{1-\zeta^2}}\\ \phi_{3,1}(t) &= \frac{\omega_{ff}}{\omega_n} g \frac{v_{ff}}{\omega_n}\mathrm{e}^{-\omega_r t}\\ &\quad\times\left(\frac{\zeta}{\sqrt{1-\zeta^2}}\sin(\omega_i t) - \cos(\omega_i t) + \mathrm{e}^{-\omega_r t}\right)\\ \phi_{3,2}(t) &= -\frac{g\frac{v_{ff}}{\omega_n}\mathrm{e}^{-\omega_r t}\sin(\omega_i t)}{\sqrt{1-\zeta^2}}\\ \phi_{3,3}(t) &= -g\left(\frac{v_{ff}}{\omega_n}\right)^2 \mathrm{e}^{-\omega_r t}\\ &\quad\times\left(\frac{\zeta}{\sqrt{1-\zeta^2}}\sin(\omega_i t) - \cos(\omega_i t) + \mathrm{e}^{-\omega_r t}\right)\\ &\quad + \mathrm{e}^{-2\omega_r t}\end{aligned} \tag{21}$$

where $\omega_r = \zeta\omega_n$ and $\omega_i = \omega_n\sqrt{1-\zeta^2}$ are introduced for the greater legibility. Note that several elements in (21) include the function found in $\phi_{2,2}(t)$. After observing that $\phi_{2,2}(t)|_{t=0} = 1$, $\dot{\phi}_{2,2}(t)|_{t=0} = 0$, and $\ddot{\phi}_{2,2}(t)|_{t=0} = -1$ it can be concluded that $-1 < \phi_{2,2}(t) < 1$ for any $\zeta \in (0, 1)$ and all $t > 0$. Another important function in (21) is:

$$\phi_s(t) = \frac{\mathrm{e}^{-\omega_r t}\sin(\omega_i t)}{\sqrt{1-\zeta^2}}. \tag{22}$$

The maximum of (22) for $t > 0$ can be obtained analytically:

$$\sup_{t>0}\phi_s(t) = \mathrm{e}^{-\frac{\zeta}{\sqrt{1-\zeta^2}}\arctan\left(\frac{\sqrt{1-\zeta^2}}{\zeta}\right)}. \tag{23}$$

If we also recall from (18) that $\omega_n^2 = \omega_{ff}^2 + g v_{ff}^2$ it can be shown after a simple analysis that for arbitrary $v_{ff} > 0$ and ω_{ff} and any choice of

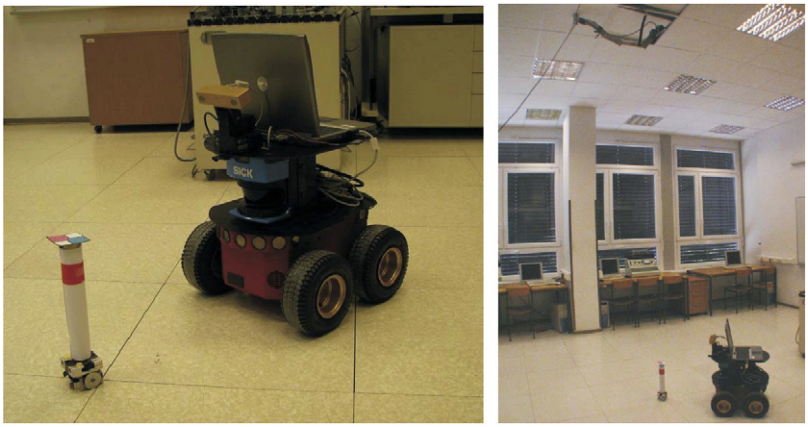

Fig. 2. Real set-up experiment: small leading robot and Pioneer 3AT with stereo camera sensor as a follower (left) and the whole set-up with top camera for trajectory tracking control of the smaller robot (right).

control law parameters $g > 0$ and $\zeta \in (0, 1)$ the following holds:

$$|\phi_{i,j}(t)| < 1 \quad t \in (0, \infty)$$
$$(i, j) \in \{(1, 1), (1, 2), (2, 1), (2, 2), (3, 3)\}. \tag{24}$$

In the following only the remaining elements of $\Phi(t)$ that can exceed 1 will be analyzed:

$$\phi_{2,3}(t) = \frac{v_{ff}}{\omega_n}\phi_{y\theta}(t), \qquad \phi_{3,2}(t) = -\frac{g v_{ff}}{\omega_n}\phi_{y\theta}(t) \tag{25}$$

$$\phi_{1,3}(t) = \frac{v_{ff}\omega_{ff}}{\omega_n^2}\phi_{x\theta}(t), \qquad \phi_{3,1}(t) = \frac{g v_{ff}\omega_{ff}}{\omega_n^2}\phi_{x\theta}(t) \tag{26}$$

with

$$\phi_{y\theta}(t) = \frac{\sin\left(\omega_n t\sqrt{1-\zeta^2}\right)}{\sqrt{1-\zeta^2}} e^{-\zeta\omega_n t}$$

$$\phi_{x\theta}(t) = \left(\frac{\zeta}{\sqrt{1-\zeta^2}}\sin\left(\omega_n t\sqrt{1-\zeta^2}\right) - \cos\left(\omega_n t\sqrt{1-\zeta^2}\right)\right) \times e^{-\zeta\omega_n t} + e^{-2\zeta\omega_n t}.$$

The maximum in (23) is also the maximum of $|\phi_{y\theta}(t)|$ for $t \geq 0$. It is the largest for $\zeta = 0$ (value of 1) and then monotonically decreases with ζ. The closed-form solution for the maximum of $|\phi_{x\theta}(t)|$ cannot be found analytically. However, it is easy to see that the maximum again decreases monotonically with ζ. It starts with 2 at $\zeta = 0$. It can be shown numerically that $|\phi_{x\theta}(t)| < 1$, $t > 0$ for $\zeta > 0.174$. The maximal values of $\frac{v_{ff}}{\omega_n}$ and $\frac{g v_{ff}}{\omega_n}$ in (25) are $1/\sqrt{g}$ and $\sqrt{g}$, respectively, and are obtained when $\omega_{ff} = 0$ (the trajectory is straight). The maximal values of $\frac{v_{ff}\omega_{ff}}{\omega_n^2}$ and $\frac{g v_{ff}\omega_{ff}}{\omega_n^2}$ in (26) are $1/(2\sqrt{g})$ and $\sqrt{g}/2$, respectively, and are obtained when $\omega_{ff}^2 = g v_{ff}^2$.

If there are many vehicles where the following vehicle tracks the path of the preceding one, it is very important that the elements of the state transition matrix are always less that 1 in magnitude. Intuitively, this will make the errors decrease along the platoon. The above analysis has shown that this could be achieved by selecting ζ high enough (at least $\zeta > 0.174$) and by selecting g close to 1. Selecting g too high will reinforce the errors from e_x and e_y to e_θ ($|\phi_{3,2}(t)|$ and $|\phi_{3,1}(t)|$ exceed 1) while selecting it too low will strengthen the error transition in the opposite direction ($|\phi_{2,3}(t)|$ and $|\phi_{1,3}(t)|$ exceed 1).

The above analysis only treated a very simplified case of a linearized model with constant reference velocities. But in practical implementation we are always faced with sensors producing noisy measurements in discrete time samples and with delay, complex trajectories, imperfect contact between the wheel and the ground etc. In the disturbance-free case the convergence of errors to 0 is achieved even if $|\phi_{i,j}(t)| > 1$ on a certain time interval. However, when the persistent modelling errors due to the difficulties mentioned above are present, these drastically influence the robot tracking capability. If $|\phi_{i,j}(t)| > 1$ on some time interval, then the persistent tracking errors are amplified by the control loop. The tracking errors thus accumulate through the platoon which can eventually lead to instability. Especially important are the discretization and the delay that add some extra phase lag in each control loop making it more oscillatory. It is virtually impossible to estimate how many robots are needed for the instability to occur since it largely depends upon bad conditions. Perhaps, it has to be stressed that the main source of the problems is usually error accumulation on e_θ to the point where controller is not continuous with respect to e_θ because of projecting it onto the interval $(-\pi, \pi]$. Even if the projection is not performed, such quick rotations of the robot make it practically useless.

5. Results of the experiment and simulations

The proposed algorithm for linear platoon control was tested on simulations and experimentally on different real mobile robot platforms.

5.1. Robot platoon using a stereo camera

The experimental environment is seen in Fig. 2 where the following robot—Pioneer 3AT (the bigger one) must follow the travelled path of the leading robot (the smaller one) considering the required safety distance L. The follower measures the distance D and the relative orientation θ_a to the leader using stereo camera sensor (Bumblebee2, Point Gray Research). The leading robot has a cylinder with red color marker attached in order to be seen by the following robot's stereo camera. The leading robot is controlled using nonlinear controller (7) to follow the reference trajectory

$$x_r(t) = 1.5\sin\left(\frac{2\pi t}{40}\right), \qquad y_r(t) = 1.1\sin\left(\frac{4\pi t}{40}\right) \tag{27}$$

where $t \in [0, 40]$ s. The tuning parameters of nonlinear control (7) for the leader are selected as $\zeta = 0.9$ and $g = 30$. The leading robot position is sensed by the camera on the ceiling (Basler A311fc, see the right part of Fig. 2).

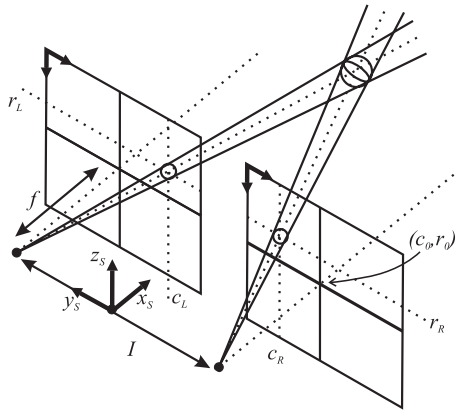

Fig. 3. Stereo camera configuration with left and right image plane.

The follower follows the path of the leading robot only by measured relative information D and θ_a to the leading robot. The position of the leading robot is not known to the follower, nevertheless it can be calculated using known D and θ_a and estimated position of the following robot using relations (8) and (9). The follower uses control law (7) to follow the reference (path of the leader) estimated using (14), the tracking error is calculated according to Eq. (5) and feed-forward control signals are calculated using relations (15) and (16). The parameters of the nonlinear control (7) for the follower are selected as $\zeta = 0.9$ and $g = 4$.

As already mentioned, the distance D and relative orientation θ_a to the leader are estimated using stereo camera sensor where the procedure is as follows: The red color marker on the leader is recognized on the left and on the right color image of the camera. Recognition is based on known color information of the marker and known size. The result of the recognition are coordinates (row r and column c) of the marker in the left and the right image frame coordinates (c_L, r_L) and (c_R, r_R), respectively. From this information and known configuration of the stereo camera shown in Fig. 3 the position of the marker in the stereo camera coordinate system [24] is obtained by

$$\begin{aligned} x_S &= \frac{If}{d} \\ y_S &= -\frac{I(c_R - c_0)}{d} - \frac{I}{2} \\ z_S &= -\frac{I(r_R - r_0)}{d} \end{aligned} \tag{28}$$

where $d = c_L - c_R$ is disparity, f is the focal distance and I is the distance between left and right camera. Finally the required relative information is obtained by $D = \sqrt{(x_S + x_{\text{off}})^2 + y_S^2}$, $\theta_a = \arctan\left(\frac{y_S}{x_S + x_{\text{off}}}\right)$, where x_{off} is the offset in x direction measured between robot frame (center of the robot) and stereo camera frame.

The results of the experiment are given in Fig. 4, where it can be seen that the leading robot follows the reference trajectory very accurately. The following robot follows the path of the leading one where smaller deviations from the leading robot path are due to odometry error position estimates, system delays, noise of stereo camera and the recognition algorithm. Due to nonholonomic constraints it is not possible to simultaneously suppress errors in orientation and in lateral direction (e_θ and e_y in relation (5)). Also the kinematics of the Pioneer 3AT mobile robot can only be approximated by kinematics of differential mobile robot type, since the wheels of the Pioneer 3AT (four wheels) must slide in order to control its orientation. When the robot needs to change its orientation its wheels need to slide on the ground and therefore the robot motion is not completely deterministic due to different grip of the wheels, dirt on the ground, etc. This, however, is a more demanding task as in differential mobile robot case. Nevertheless, the following robot can follow the leading robot satisfactorily (left part of Fig. 4) with maintaining the safety distance (right part of Fig. 4) which is close to the required one ($L = 0.6$ m). The control signals for the leading robot and the following robot are shown in Fig. 5. The control signals contain some noise which is again due to the influence of different noise sources, sensors, wheel slipping and the like.

5.2. Simulations of a large platoon

The effect of error propagation through the number of robots in the platoon analyzed in Section 4 is demonstrated by simulating the platoon of a large number of differential robots. Two different platoon approaches were simulated and compared, namely constant inter-vehicle distance and constant inter-vehicle time delay. In both cases the platoon control strategy is as proposed in Section 3. The leading robot is controlled using nonlinear controller (7) to follow the reference trajectory

$$x_r(t) = 0.5 \sin\left(\frac{2\pi t}{30}\right), \qquad y_r(t) = 0.5 \sin\left(\frac{4\pi t}{30}\right) \tag{29}$$

where $t \in [0, 30]$ s. The tuning parameters of nonlinear control (7) for the leader and the follower robots are selected as $\zeta = 0.9$ and $g = 50$.

Resulting trajectories of an eight-robot platoon with constant distance approach are shown in Fig. 6. Here it can be seen that robot trajectories diverge from the reference trajectory although no noise and initial posture errors are present. This is also seen from the table of summed squared tracking errors (Table 1).

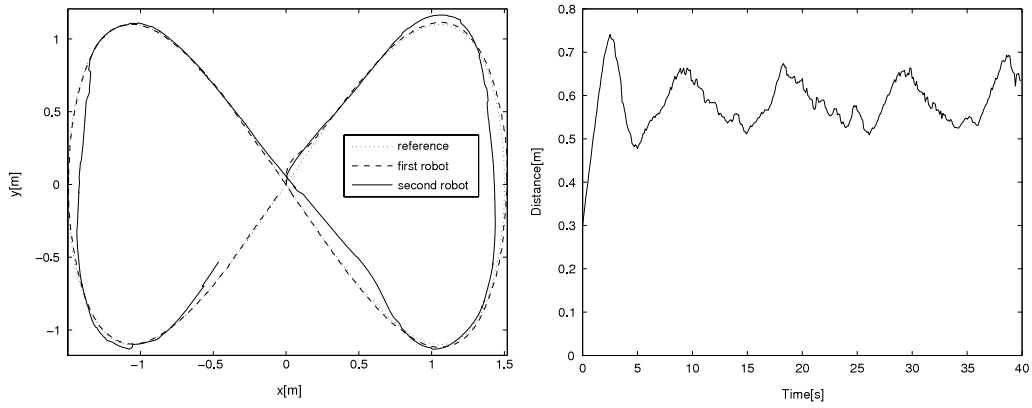

Fig. 4. Results of the experiment with two real robot platoon: robot's trajectory (left) and distance between the robots (right).

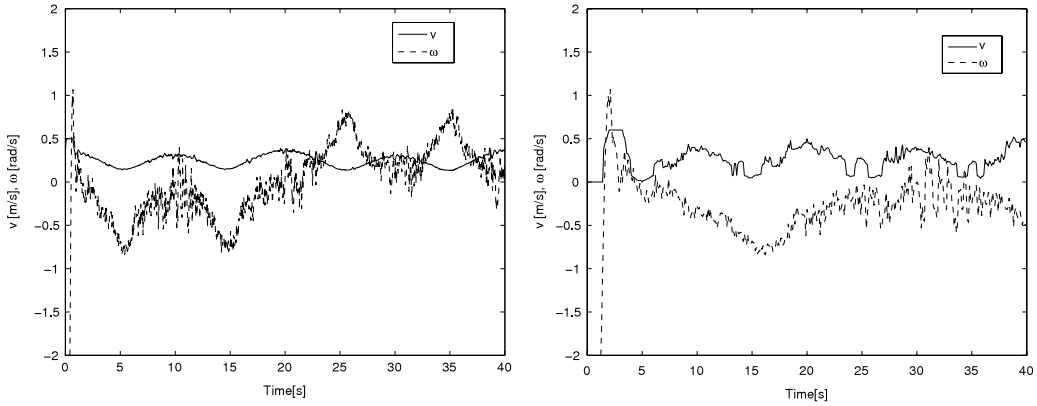

Fig. 5. Tangential and angular velocity for the leading robot (left) and for the following robot (right).

Table 1
Comparison of the sum of the squared tracking errors over the whole path and for each robot in the platoon.

Approach	SSE_1	SSE_2	SSE_3	SSE_4	SSE_5	SSE_6	SSE_7	SSE_8	SSE_9	SSE_{10}
const. distance	0.342	2.548	2.768	4.075	6.388	8.260	8.340	9.641	–	–
const. time	0.342	0.682	1.048	1.415	1.706	1.957	2.199	2.437	2.678	2.920

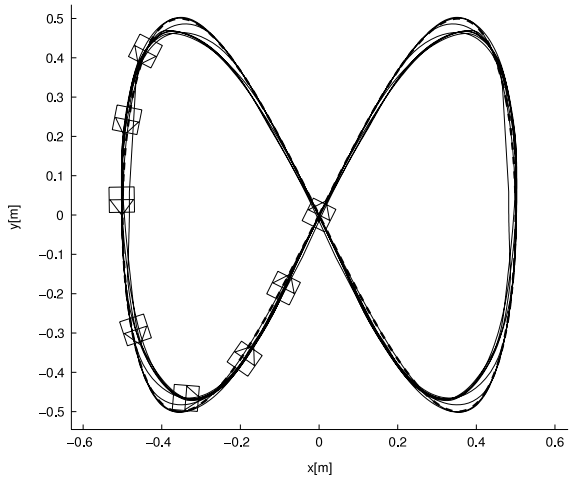

Fig. 6. A platoon of eight robots using constant inter-vehicle distance ($L = 0.2$ m). Reference trajectory is shown with a dashed line.

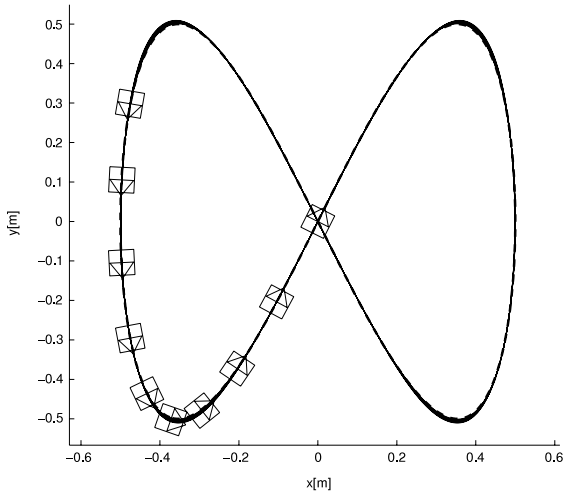

Fig. 7. A platoon of eight robots using constant inter-vehicle time ($T_f = 1$ s). Reference trajectory is shown with a dashed line.

Nevertheless constant vehicle spacing platoon results are still usable for a limited number of robots (eight in our case). If adding additional robots (nine or more), the resulting behaviour of those additional robots is unstable.

Resulting trajectories of a ten-robot platoon with constant time approach are shown in Fig. 6. Here it can be seen that all ten robots drive much closer to the reference trajectory as in the constant distance case which is also seen in a smaller error accumulation in Table 1. The robots inter-vehicle distance here varies with the robot speed—the higher the speed, the higher the distance among them. Usually speed profile is selected to adapt to the trajectory curvature. When curvature is high, the speed is low and vice versa. This enables a better trajectory tracking because the speed is lower in curvy parts and the used controller (7) dynamics can follow trajectory better (see Fig. 7).

6. Conclusion

A local control strategy for the control of vehicle platoons is proposed where the following vehicle only has information about its own orientation and about the distance and azimuth of the leading vehicle. Its own position is determined using odometry. It calculates the reference path in a parametric polynomial form, and the parameters of the polynomials are determined by the least-squares method. Having the reference path, the feed-forward and feed-back control are applied to the following vehicle. The proposed algorithm was tested on an experimental set-up consisting of two different mobile robot types: a differential two-wheel robot and an outdoor four-wheel robot. The objective of the experiment and simulation analysis is to demonstrate the ability of the proposed algorithm to effectively drive vehicles in a platoon with either constant inter-vehicle distance or constant inter-vehicle time approach. Constant time approach is more appropriate for a large number of vehicles platoon due to slower error accumulation. This confirms the theoretical results from the literature.

The analysis of error accumulation was also performed. The results have shown the increase of error with the increasing number of vehicles in the platoon. In the case of a long train of vehicles another problem occurs, namely string stability. The maximum number of vehicles that still enables a satisfactory behaviour depends on many factors such as level of noise in measurements, delay in measurements, discretization time, shape

of trajectories, unmodelled dynamics, wheel slipping and control parameters. Some guidelines on choosing the appropriate control parameters are given in the paper.

References

[1] J. Hedrick, M. Tomizuka, P. Varaiya, Control issues in automated highway systems, IEEE Control Systems Magazine 14 (6) (1994) 21–32.
[2] P. Ioannou, Z. Xu, Throttle and brake control systems for automatic vehicle following, IVHS Journal 1 (4) (1994) 345–377.
[3] P. Daviet, M. Parent, Longitudinal and lateral servoing of vehicles in a platoon, in: IEEE Intelligent Vehicles Symposium Proceedings, 1996, pp. 41–46.
[4] J.J. Moskwa, J.K. Hedrick, Nonlinear algorithms for automotive engine control, IEEE Control Systems Magazine 10 (3) (1990) 88–93.
[5] S. Sheikholeslam, C.A. Desoer, Longitudinal control of a platoon of vehicles with no communication of lead vehicle information: a system level study, IEEE Transactions on Vehicular Technology 42 (4) (1993) 546–554.
[6] H. Lee, M. Tomizuka, Adaptive vehicle traction force control for intelligent vehicle highway systems (IVHSs), IEEE Transactions on Industrial Electronics 50 (1) (2003) 37–47.
[7] H. Fritz, Longitudinal and lateral control of heavy duty trucks for automated vehicle following in mixed trafic: experimental results from the Chauffeur project, in: IEEE Conference on Control Applications—Proceedings, vol. 2, 1999, pp. 1348–1352.
[8] M.J. Woo, J.W. Choi, A relative navigation system for vehicle platoon, in: SICE 2001, Proceedings of the 40th SICE Annual Conference, International Session Papers, 2001, pp. 28–31.
[9] J.-M. Contet, F. Gechter, P. Gruer, A. Koukam, Application of reactive multiagent system to linear vehicle platoon, in: Annual IEEE International Conference on Tools with Artificial Intelligence, ICTAI, 2007, pp. 67–70.
[10] S.K. Gehrig, F. Stein, Elastic bands to enhance vehicle following, in: IEEE Conference on Intelligent Transportation Systems, Proceedings, ITSC, 2001, pp. 597–602.
[11] S.-Y. Yi, K.-T. Chong, Impedance control for a vehicle platoon system, Mechatronics (UK) 15 (5) (2005) 627–638.
[12] S. Halle, B. Chaib-draa, A collaborative driving system based on multiagent modeling and simulations, Transportation Research Part C (TRC-C): Emerging Technologies (UK) 13 (4) (2005) 320–345.
[13] H.S. Tan, J. Guldner, C. Chen, S. Patwardhan, B. Bougler, Lane changing with look-down reference systems on automated highways, Control Engineering Practice 8 (9) (2000) 1033–1043.
[14] Y. Zhang, E.B. Kosmatopoulos, P.A. Ioannou, C. Chien, Autonomous intelligent cruise control using front and back information for tight vehicle following maneuvers, IEEE Transactions on Vehicular Technology 48 (1) (1999) 319–328.
[15] J. Fredslund, M. Matarić, A general algorithm for robot formations using local sensing and minimal communications, IEEE Transactions on Robotics and Automation 18 (5) (2002) 837–846.
[16] J. Cortés, S. Martínez, T. Karatas, F. Bullo, Coverage control for mobile sensing networks, IEEE Transactions on Robotics and Automation 20 (2) (2004) 243–255.
[17] J. Bom, B. Thuilot, F. Marmoiton, P. Martinet, A global control strategy for urban vehicles platooning relying on nonlinear decoupling laws, in: Proceedings of the 2005 IEEE/RSJ International Conference on Intelligent Robots and Systems, 2005, pp. 1995–2000.
[18] C.Y. Liang, H. Peng, Optimal adaptive cruise control with guaranteed string stability, Vehicle System Dynamics 31 (1999) 313–330.
[19] G. Klančar, D. Matko, S. Blažič, Wheeled mobile robots control in a linear platoon, Journal of Intelligent and Robotic Systems 54 (5) (2009) 709–731.
[20] G. Oriolo, A. Luca, M. Vandittelli, WMR control via dynamic feed-back linearization: design, implementation, and experimental validation, IEEE Transactions on Control Systems Technology 10 (6) (2002) 835–852.
[21] A. Luca, G. Oriolo, M. Vendittelli, Control of wheeled mobile robots: an experimental overview, in: S. Nicosia, B. Siciliano, A. Bicchi, P. Valigi (Eds.), RAMSETE—Articulated and Mobile Robotics for Services and Technologies, Springer-Verlag, London, 2001.
[22] M. Fliess, J. Levine, Ph. Martin, P. Rouchon, Flatness and defect of nonlinear systems: introductory theory and examples, International Journal of Control 61 (6) (1995) 1327–1361.
[23] C. Samson, Time-varying feedback stabilization of car-like wheeled mobile robots, International Journal of Robotics Research 12 (1) (1993) 55–64.
[24] S. Se, D.L.J. Little, Mobile robot localisation and mapping with uncertainty using scale-invariant visual landmarks, The International Journal of Robotics Research 21 (8) (2002) 735–758.

Gregor Klančar received the B.Sc. and Ph.D. degrees in 1999, and 2003, respectively, from the Faculty of Electrical Engineering of the University of Ljubljana, Slovenia, where he is currently employed as an assistant professor. His research interests are in the area of fault diagnosis methods, multiple vehicle coordinated control and mobile robotics.

Drago Matko received the B.Sc., M.Sc. and Ph.D. in electrical engineering in 1971, 1973 and 1977 respectively, from the University of Ljubljana, Slovenia for work in the field of Adaptive control systems. He visited the Institute for Control Engineering Darmstadt, Germany several times, during 1980–82, 1984, 85 and 86 as a Humboldt fellow, during 1987–91 in the frame of the project Adaptive control systems sponsored by International Bureau KFA Jülich. He visited the Institute of Space and Astronautical Science in Sagamihara Kanagawa, Japan as a Foreign Research Fellow for 9 months during 1995–96 and for 6 months during 2003–04. He has published 47 journal articles, more than 200 conference papers and four student edition books (in Slovene) and he is also coauthor of two books published by Prentice Hall. He received the award of Slovenian ministry for research and technology for the work in the field of computer aided design of control systems in 1989 and Zois award for achievements in science in 2003.

Sašo Blažič received the B.Sc., M. Sc., and Ph. D. degrees in 1996, 1999, and 2002, respectively, from the Faculty of Electrical Engineering, University of Ljubljana. His research interests include adaptive, fuzzy and predictive control of dynamical systems and modelling of nonlinear systems. He is also working in the area of mobile robotics with a stress on path planning and path following issues.